

## ENERGY PRODUCTION AND SANITATION IMPROVEMENT USING MICROBIAL FUEL CELLS

Oliver Knoop<sup>a</sup>, Debbie Lewis<sup>b</sup>, John Greenman<sup>c</sup> and Ioannis Ieropoulos<sup>b\*</sup>

<sup>a</sup> Universität Duisburg-Essen, Germany, <sup>b</sup> Bristol Robotics Laboratory, University of the West of England and University of Bristol, UK, <sup>c</sup> Centre for Research in Biosciences, University of the West of England, Bristol, UK. \* Corresponding author details Bristol Robotics Laboratory, University of the West of England and University of Bristol, T-Building, Frenchay Campus, Coldharbour Lane, BS16 1QY, UK; Tel: 044 117 3286318; Fax: 044 117 3283960; email: [ioannis.ieropoulos@brl.ac.uk](mailto:ioannis.ieropoulos@brl.ac.uk); website: <http://www.brl.ac.uk/>.

**Comment [i1]:** I think the authors' list, affiliations etc has to be the same as on the Abstract (same with the title).

**Comment [i2]:** Debbie, Oliver – please confirm.

**ABSTRACT (Note for Conference full paper layout length 200-500 words but if accepted IWA requires only 100-200 words)**

*The potential for Microbial Fuel Cell (MFC) technology to utilise wet organic waste products (including human urine) has been previously reported in the scientific literature. Preliminary findings from the study of a collection of small scale MFCs, working both as individual units in cascade or collectively as an interconnected stack utilising artificial urine, are reported. This is part of a larger study that is investigating the potential of the MFC technology to generate energy whilst treating urine waste as well as produce clean water and render any pathogens that might be present. Artificial urine was prepared from pure chemical components at concentrations typically found in real urine. MFCs were constructed from Nanocure® resin polymer using rapid prototype technology. The anode and cathode electrodes were made of carbon veil material with 15cm<sup>2</sup> total surface area, folded down to fit in the small 1mL chambers. A total of 8 MFC were inoculated using activated anaerobic sludge; after 17 days of fed batch mode they were switched to continuous flow, initially at low flow rates (0.09 ml h<sup>-1</sup>) and subsequently at higher rates (up to 1ml h<sup>-1</sup>), resulting in HRT of 6.4 minutes/MFC. MFCs showed stable performances following the maturing period and produced, under polarisation experiments, peak power output levels of the order of 39.6µW which corresponds to 39.6W/m<sup>3</sup> (normalised value). Data from continuous flow experiments showed higher power production, increasing with the concentration of the C/E source within artificial urine. The work has demonstrated that artificial urine of varying composition can be successfully utilised for the production of energy, whilst treating (cleaning-up) the urine stream. The next stage of this work will be to interconnect the MFCs into a stack and envisage practical applications such as digital wristwatches, LEDs and small motors.*

**Comment [DL3]:** Will update when happy with the rest.

**Comment [i4]:** Yep ok.

Keywords: urine, microbial fuel cells, sanitation, waste utilisation, practical application

### INTRODUCTION

Microbial Fuel Cells (MFCs) are unique bio-electrochemical transducers that convert wet organic waste directly into electricity, through the metabolism (waste treatment) of constituent microorganisms. One such global and abundant waste product is human or animal urine, which has already been demonstrated to be an efficient fuel for direct electricity production via single MFCs with >50% efficiency (Ieropoulos, Greenman & Melhuish, 2012). The MFC is a true green technology that operates within the immediate carbon cycle and does not rely on fossil fuels, but it also carries the added advantage of low cost in manufacture and maintenance. MFCs may therefore provide a solution for delivering a sustainable energy

source for the future, whilst concomitantly providing clean water production, advantageous for developed and developing countries (Ieropoulos, Greenman & Melhuish, 2008,12).

Improved energy outputs and scale-up of the technology are most likely to be achieved through miniaturisation and multiplication of MFC units and thus careful fine tuning of the key parameters governing the performance of stacks of miniaturised MFCs, is critical (Ieropoulos, Greenman & Melhuish, 2008; Qian & Morse, 2011; Fangzhou *et al.*, 2011; Ieropoulos, Greenman & Melhuish, 2010b). Some of the parameters that have already been considered include the inoculum source and community mix (Zhang *et al.*, 2012b, 2012a; Ieropoulos, Winfield & Greenman, 2010b); substrate (Futamata *et al.*, 2012; Yu *et al.*, 2012); catholyte (Zhang *et al.*, 2012a; Harnisch & Schröder, 2010); MFC structural material (Ieropoulos, Greenman & Melhuish, 2010b); flow rate (Winfield, Ieropoulos & Greenman, 2012; Ledezma, Greenman & Ieropoulos, 2012; Ieropoulos, Winfield & Greenman, 2010b); anode material (Liu *et al.*, 2012; He *et al.*, 2012); anode chamber volume to electrode surface area (Ieropoulos, 2006) and the type of proton exchange membrane (Ieropoulos, Greenman & Melhuish, 2010b).

The overall aim of our work was to investigate the performance of novel small scale MFCs (2mL volume) assembled in a stack configuration and fed with artificial urine and demonstrate their practical implementation by directly powering electronic devices. The stack was configured in a cascade manner, where all MFC units were hydraulically linked, in an attempt to sequentially treat the urine fuel at different added carbon-energy concentrations and thus better utilise the organic contents. Several other key parameters were investigated for improving the energy output and two electronic devices were powered; LEDs and a dc motor driving a toy windmill.

## MATERIALS AND METHODS

### Inoculum source and set-up

Anaerobic activated sewage sludge was provided by the Wessex Water Scientific Laboratory, (Saltford, UK). Samples were initially kept in their original water-based suspension at 4 ° and stored for 3 months. Prior to the experiments, sludge samples were mixed with 1% tryptone, 0.5% yeast extract (Oxoid, Basingstoke, UK) and allowed to acclimatise at room temperature before inoculating the whole connected stack (8 MFCs) with 20 ml of sludge added through the inflow of MFC 1 and allowed to flow downstream. Once all 8 units were inoculated, the system was kept in batch mode for X days/weeks (fig. 1).

Comment [115]: Oliver?

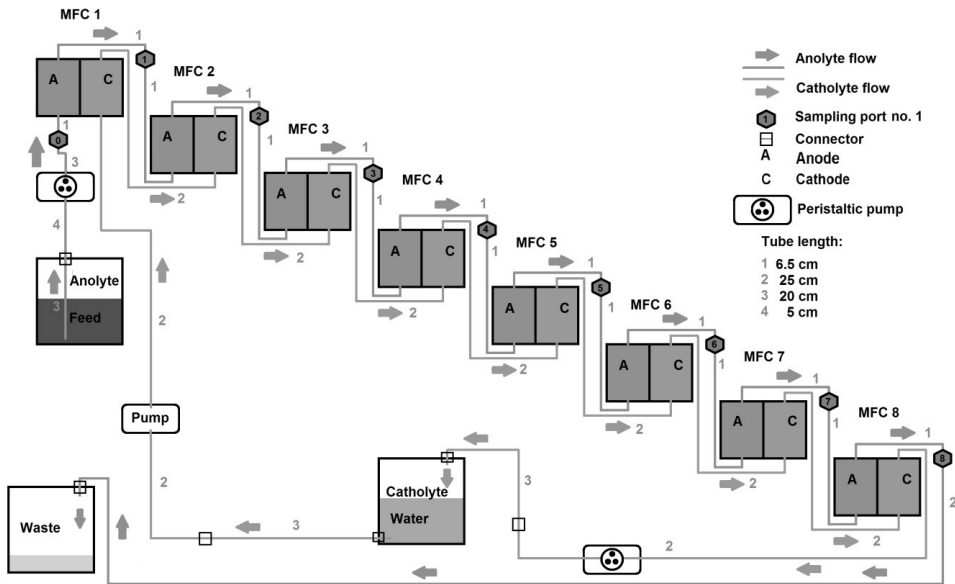


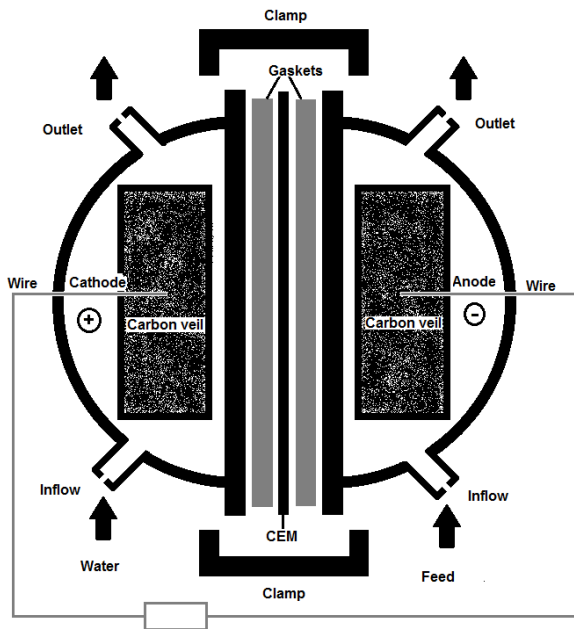
Figure 1. Set-up of 8 MFC as a cascade.

The initial inoculum was replaced on days 3, 6, 7, 8, 9, 10, 13 and 14 in the same manner. On day 18, the stack was fed with artificial urine medium (AUM) as described by Brooks & Keevil (1997) with the exception of tetrasodium pyrophosphate added at a concentration of 0.006g/l to prevent precipitation (Sigma-Aldrich, Dorset, UK). AUM was then filter sterilised with a 0.2  $\mu\text{m}$  filter (Merck Millipore, Ireland). AUM was fed initially on a continuous flow rate of 0.086 ml/h to the MFC stack using a peristaltic pump (Waston Marlow 101 U/R). On day 21 (from the initial inoculation) this was increased to 0.43 ml/h. On day 23, the AUM was supplemented with an additional 9 g/l of peptone and 4.995 g/l yeast extract (AUM 10x) to accelerate the growth of the anodophilic microorganisms.

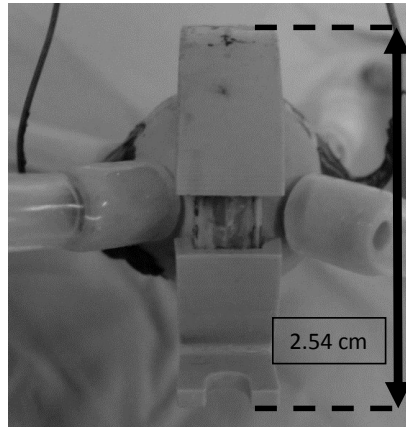
Tap water was used as the catholyte, recirculated by a different peristaltic pump (Welco WPX 1, Japan) and controlled with a DC regulated power supply (DPS-1850, Manson, UK) at a flow rate of 298.27 ml/h. The water was consistently exchanged every 7 days.

#### Small-scale MFC design

The 8 small-scale MFCs were designed using the SolidEdge® CAD software and fabricated using rapid-prototype 3D-printing (Perfactory® technology). The structural material used was the RCP23 (Nanocure®) resin, doped with ceramic nanoparticles. Anode and cathode chambers were designed to have a total volume of 1 ml, and were separated by a cation-exchange membrane (CEM) for proton transfer (CMI-7000S, Membranes International Inc, USA). Carbon veil electrodes of 15  $\text{cm}^2$  (30  $\text{g}/\text{m}^2$ ; PRF Composite Materials, UK) were inserted in each half-cell. Gaskets (O-rings) were used on either side of the membrane for water tightness, and were produced from two elastic compounds in equal amounts that were allowed to air-dry and cure into 2 mm thickness films (Plasti Gel 00 (A & B), Mouldlife Materia Innovation, UK). Figure 2 shows a schematic and side-view photo of the small-scale MFC.



b)



a)

Figure 2. a) Schematic diagram of the small-scale MFC and b) Photograph of an actual small-scale MFC. Total height is 2.54 cm.

#### Conductivity of the different media.

The different concentrations of AUM were diluted at a ratio of 1:8 in distilled water and the conductivity of these was measured by a portable multi-parameter (HI991300 with a HI 1288 electrode, HANNA Instruments LTD, UK). The same apparatus was used for determining the conductivity of the tap water catholyte.

#### Data capture and calculations of power output.

Electrode output was recorded in volts (V) against time by using an ADC-16 Channel Data Logger (Pico Technology Ltd, Cambridgeshire, UK). Power output was calculated as described by Ioannis Ieropoulos, Winfield, & Greenman (2010).

#### Polarisation experiments.

Polarisation experiments were performed using a load-controlled measurement tool as described by (Degrenne, N., Buret, F., Allard, B., Bevilacqua, 2012). The resistor range was from 38.4 k $\Omega$  to 3.74  $\Omega$  and controlled with the Bio-Electrical Energy Management Software (v 1.0.6, Laboratoire AMPERE, Février, 2012). The time step for each resistor load connected to the MFCs was 3 minutes and the data were recorded every 30 seconds. Polarization experiments were performed for a variety of substrates based on the AUM recipe (AUM 2 x was supplemented with an additional 1 g/l peptone and 0.005 g/l yeast extract and AUM 5 x with an additional 4 g/l peptone and 0.02 g/l yeast extract). The flow rate was kept constant

at 0.450 ml/h throughout all the experiments. Prior to polarisation experiments, all MFCs were left open circuit ( $V_{oc}$ ) for X hours, to obtain steady state values.

### Electrical Stack Configurations

Four different electrical configurations were tested for the stack of 8 MFCs, namely series, parallel and two variants of series-parallel combinations; 4 groups of 2-in-parallel MFCs, connected in series (termed "4(2)-series") and 2 groups of 4-in-parallel MFCs connected again in series (termed "2(4)-series"). This was in order to derive the best performing configuration for powering the electronic devices.

### Practical implementation

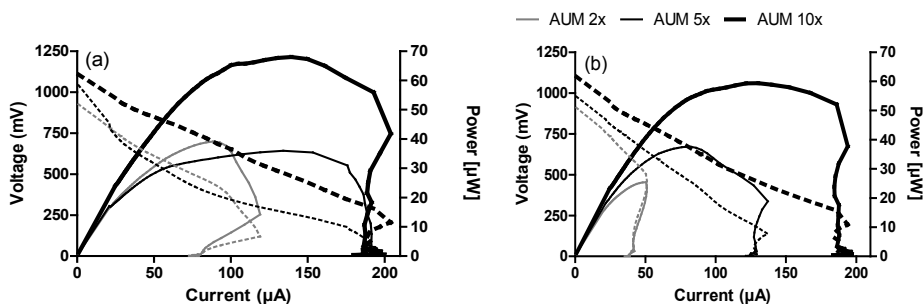
A windmill model (SOL-EXPERT group, Ravensberg, Germany) was used as an exemplar of a dc motor. The solar panel was disconnected and the MFC stack was connected instead, via two capacitors (X Farads, DCNQ; Illionois Capacitors Inc, USA). The capacitors were used to accumulate the energy from the MFCs and therefore step it up, in order to match the power requirements of the windmill dc motor, similar to the EcoBots (Ieropoulos et al., 2003; Melhuish et al., 2006; Ieropoulos et al., 2010).

Comment [i6]: Oliver?

## RESULTS AND DISCUSSION

### Characterisation of small-scale MFCs within a cascade with increasing C/E source.

Figure 3(a-d) shows the polarisation and power curves for MFC 1, 4, 5 and 8 respectively performed over a one-week period with increasing concentrations of C/E (peptone and yeast extract) added to the AUM fuel. Each polarisation sweep was performed two days after a change of substrate. With AUM 10x as the anolyte, MFC1 produced the highest power of 67  $\mu$ W with decreasing values for in order of the downstream MFC position, with MFC 8 producing the lowest power of 47 $\mu$ W. For all MFCs the polarisation curves showed, that the fuel cells were mainly limited by mass transfer losses, whereas nearly no activation losses were found. By reducing the amount of peptone and yeast extract in the anolyte, the mass transfer losses occurred sooner, ultimately limiting the power generation. The power curves for AUM 2x in figure 3 (b-d) indicate an 'overshoot' trend for all MFCs, which tends to rise to a higher power, but then rapidly decrease in both current and voltage terms. In MFC 5 for AUM 5x (fig. 3c) the MPP was not directly limited by this type of loss, however this was the case for the MFCs further downstream; MFC 6, 7 (data not shown), and MFC 8 (fig. 3d).



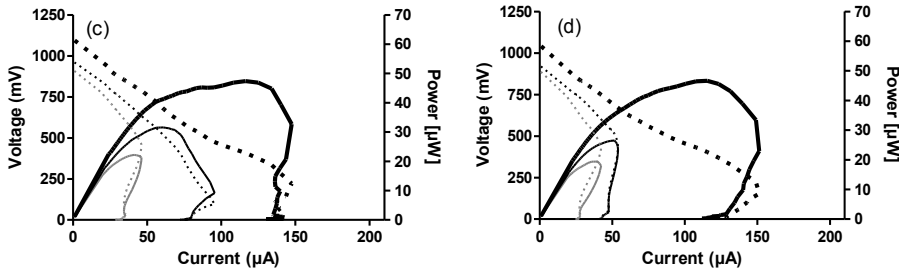


Figure 3. Polarization (left y-axis/dashed lines) and power (right y-axis/solid line) curves for MFC 1 (a), MFC 4 (b), MFC 5 (c) and MFC 8 (d).

The sequential downstream decrease in power is shown in Figure 4a, which was more marked when the fuel cells were fed AUM 10x. Decreasing maximum power points (MPPs) in the numerical order of the cascade, can be explained by the reduction of available nutrients by the preceding MFC, thus resulting in more dilute influents reaching the downstream MFCs. With AUM 5x and AUM 2x significantly lower MPPs were obtained and the polarisation curves showed that mass transfer losses were dominant and therefore limiting the performance, with more marked effects for the downstream MFCs. The findings for different nutrient concentrations are in agreement with previous studies on small-scale MFC cascades (Winfield, Ieropoulos & Greenman, 2012).

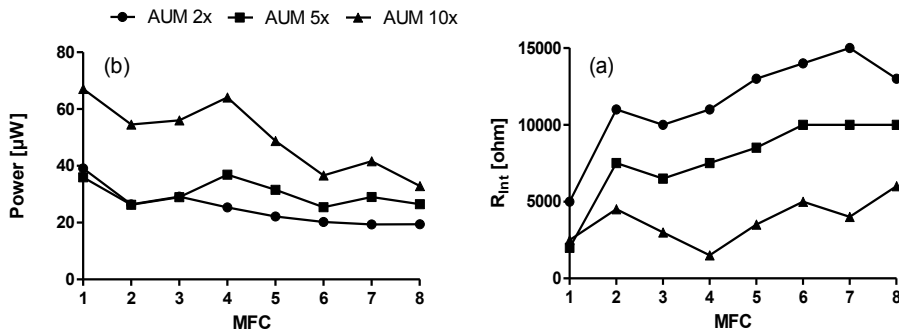


Figure 4. MPP (a) and internal resistance (b) of each MFC in the cascade whilst fed AUM 2x, 5x and 10x.

Figure 4b. illustrates the behaviour of the internal resistance for MFCs 1 to 8 for all three substrates, which may help explain the decreasing power performance. As can be seen, with increasing concentrations of nutrients, the internal resistance of each MFC was reduced, which was likely due to the increase in conductivity of the anolyte (see Table 1).

	Tap water	AUM 2x	AUM 5x	AUM 10x
Conductivity [μS/cm]	800	24,048	25,216	26,440

Table 1. Conductivity of the anolyte AUM 2x, 5x, and 10x and of tap water (catholyte).

### Effects of high nutrient concentration (AUM 10x) over time

To determine the effect of increasing the available nutrients on the development of the anodic biofilm the cascade was fed for 6 days with AUM 10x with polarisation experiments performed on days 2, 4 and 6. Figure 5 shows the development of the MPPs (a) and the internal resistance (b) for the period of 6 days.

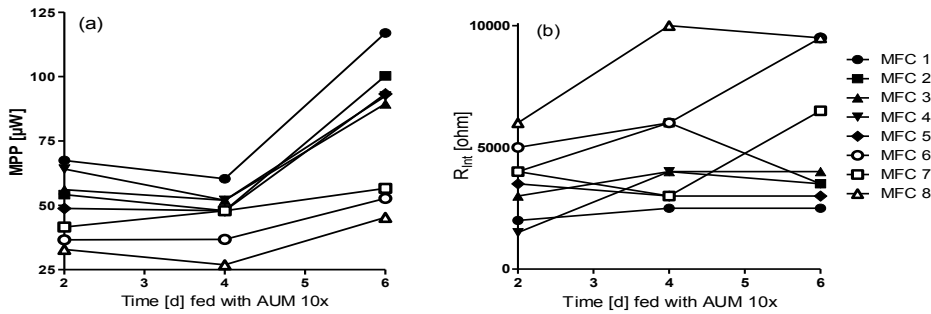


Figure 5 MPP (a) and internal resistance (b) of each MFC in the cascade over 6 days fed with AUM 10x.

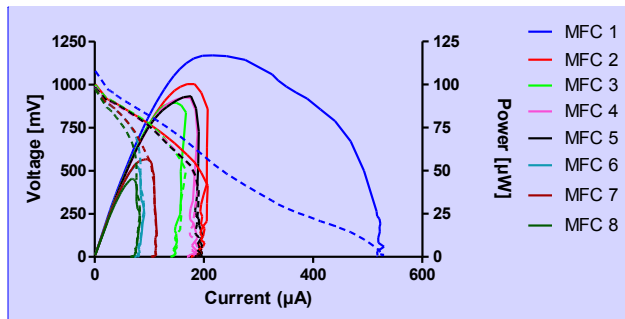
As can be seen, the MPP increases with time for all MFCs (see fig. 5b), however the rate of increase for the further downstream MFCs 6-8, is lower than that of MFCs 1-5. This is reflected in the higher increases in internal resistance for MFCs 6-8 (Figure 5b), compared to very little increases during the first 4 days and almost no increase between days 4-6 for MFCs 1-5. The increasing internal resistance in cascades had been previously described by Winfield, Ieropoulos & Greenman (2012). The constant behaviour of the MFCs 1-5 internal resistance was expected as a result of the more enriched and more conductive influent reaching those units first.

### Maximum power output

The highest power recorded within this work by a single small-scale MFC 1 was 116.96  $\mu\text{W}$ , (power density 116.96  $\text{W}/\text{m}^3$ - total anode chamber volume; 77.97  $\text{mW}/\text{m}^2$  - total surface anode area), fed with AUM 10x for 6 days, as shown in Table 2. As can also be seen in Figure 6, MFC1 also showed negligible mass transfer losses and the lowest internal resistance compared to all the other MFCs in the cascade.

	actual power	Power Density $P_D$				
	P [ $\mu\text{W}$ ]	$P_{D, SA}$ [ $\text{mW}/\text{m}^2$ ]	$P_{D, PSC}$ [ $\text{mW}/\text{m}^2$ ]	$P_{D, TV}$ [ $\text{W}/\text{m}^3$ ]	$P_{D, EV}$ [ $\text{W}/\text{m}^3$ ]	$P_{D, EV}$ [ $\text{W}/\text{L}$ ]
MFC 1 (best)	116.96	77.97	974.66	116.96	962.94	0.96
average	80.87	53.91	673.93	80.87	849.40	0.85

Table 2. : Maximum and average absolute power P and normalized power density  $P_D$  for MFC1. Power density was normalized based on the total surface anode area (SA), projected surface area of the cathode (PSC), total anode chamber volume (TV)(Ieropoulos, Greenman & Melhuish, 2010b), and anode chamber exchange volume (EV)(Logan, 2012).



**Comment [i7]:** Oliver, perhaps you can split it a power curves graph and a separate polarisation curves graph, side by side, please

Figure 6. Polarisation ( - - - ) and power curves ( — ) 6 days after the anolyte of the cascade was changed to AUM 10x.

The power output produced by MFC1 is higher than that reported for MFCs with comparable anode chamber volumes, however the experimental conditions were significantly different, in terms of the anode electrode surface area, cathodic half-cell and anolyte flow rate (Ieropoulos, Greenman & Melhuish, 2010c; Winfield, Ieropoulos & Greenman, 2012). It can therefore be assumed that the low exchange volume of the MFCs in the current study as a result of the bigger anode electrode, the highly concentrated substrate and the low HRT of approximately 12.7 min might have assisted in overcoming the diffusion limitations due to the advective flow in MFC1. The high MPP might also be an indicator for conditions of electron spilling by the anodophilic organisms (Russell, 2007).

#### Production of Constant Power

To confirm that each stage of the cascade can produce a constant power over time, the output of all 8 MFCs were monitored with two different loads (10 k $\Omega$  and 3.3 k $\Omega$ ) over a period of 39 hours after initial stabilisation. As can be seen in Figure 7, less divergence was recorded between the MFCs for the higher load (10 k $\Omega$ ). Nevertheless, the order of the produced voltages for each MFC in both graphs corresponds to their position in the cascade with the exception of MFC 6 at the lower load.

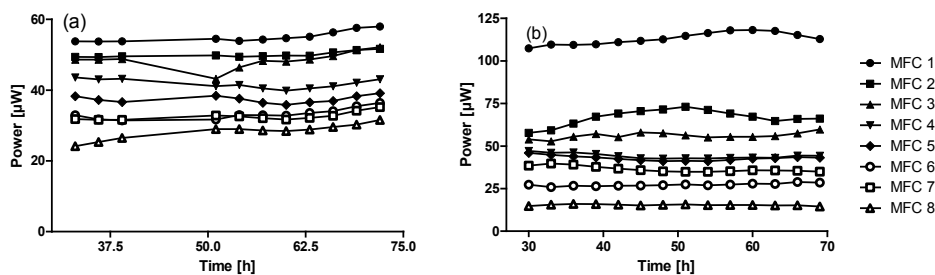


Figure 7. Power levels measured over a period of 39 hours with a 10 k $\Omega$  (a) and a 3.3 k $\Omega$  (b) load, after stabilisation of the voltages (substrate AUM 10x).

The average power produced per MFC was 40.86  $\mu$ W under 10k $\Omega$  loads and 50.26  $\mu$ W under 3.3k $\Omega$  loads. Under the 10k $\Omega$  load, MFC1 produced 55.07  $\mu$ W (highest) whereas MFC8 produced 28.27  $\mu$ W (lowest), which was 51.2%. With the 3.3k $\Omega$  load MFC8 produced 15.36  $\mu$ W, which is equal to 13.6 % of the highest power produced by MFC 1 (113.18  $\mu$ W).

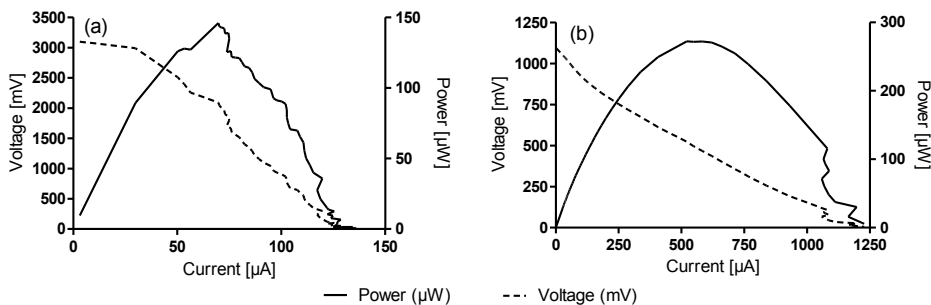


These results therefore suggest that a decreasing performance in downstream MFCs is more pronounced as heavier loads are applied. This indicates a relationship between metabolic rate and applied load, since increased metabolism in upstream MFCs results in a decreased nutrient supply in downstream MFCs. Relationships like this can be exploited in stack design and development for dynamic *in-situ* adjusting and reconfiguration.

### Electrical Stack

Polarisation experiments were performed for the different stack connections in order to find the best performing configuration to operate the practical applications. The polarization and power curves are shown in Figure 8 as follows: (a) "series"; (b) "parallel"; (c) "2(4)-series" and (d) "4(2)-series". Figure 8 (a) shows that the open circuit voltage of all MFCs connected in series was 3.1V, which is approximately one third of the sum for all the individual MFC voltages (9 V – data not shown). The polarisation curve shows, that the ohmic losses were dominant and thus the main limitation of performance for this configuration. The lower than the theoretical maximum open circuit voltage and the severe ohmic losses under the series condition can be explained by the 'short-circuit' effect of the fluidic links between the MFCs in the cascade, which provide an alternative path for electrons to flow. Fluidic isolation between MFCs has been previously reported as a critical factor in stacks (Ieropoulos et al. 2008; 2010b), however the objective of sequential artificial urine treatment in the current study, could only be achieved through fluidic linkage between all MFCs. The all in series configuration was nevertheless a valuable test to reveal the degree of losses from such a sub-optimal (in electrical terms) arrangement.

The open circuit voltage of the stack configuration in "parallel" was as expected 1.1V, which is the mean of the individual MFCs open circuit voltage ([Error! Reference source not found. figure 8 \(b\)](#)). This configuration produced a maximum current of 1.227 mA and the highest MPP (271  $\mu$ W at 574  $\mu$ A), but the lowest operating voltage at the MPP (495 mV).



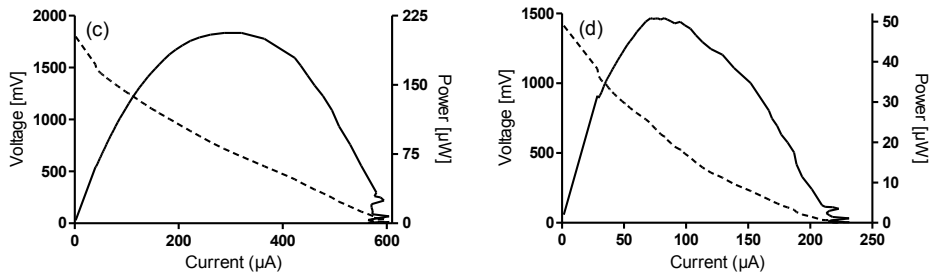


Figure 8. Power and polarization curves for the stack configurations: (a) series; (b) parallel; (c) "2(4)-series"; (d) "4(2)-series".

To reach practically useful power outputs the results in Figure 8 show that it was necessary to use a combined series/parallel configuration of 2 groups of 4-in-parallel MFCs, connected in series (fig. 8c), which showed the best combination of voltage (642 mV), current (312  $\mu$ A) and power 206  $\mu$ W (2010a as well) (Winfield, Ieropoulos & Greenman, 2012).

#### Practical implementation: LED and dc-motor powered windmill

To show the feasibility of MFCs to power real applications, the stack configuration "series" was used to operate a red LED. The LED was successfully operated constantly at a voltage of 1.63 V, with a 40  $\mu$ A current consumption by the LED (video documentation is available upon request).

To successfully operate the more energy demanding small wooden windmill, the MFCs were configured in the "2(4)-series", that charged the  $X$  Farads capacitors from 20 mV to 780.90 mV, over a period 280 min. The process of charging the capacitors was monitored and is shown in Figure 9. The slope of the graph represents the rate of charging, which is equal to the amount of current produced. This rate is shown to decrease as voltage increases, which is the result of the dielectric properties of capacitors (Duncan, 1997). The windmill was operated with from the charged capacitors for 217 seconds and the motor stopped moving at a voltage of 171mV (video documentation is available upon request).

Comment [i8]: Oliver?

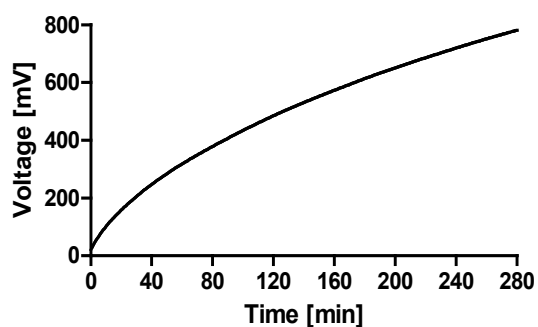


Figure 9. Charging of the two capacitors by the cascade in configuration "2(4)-series".

## CONCLUSIONS

The experiments presented in this paper have demonstrated the utilisation of artificial urine in novel 2mL small scale MFCs for power generation. By increasing the amounts of carbon/ energy concentration in the AUM the power generation of all of the MFCs within the cascade increased, in relation to their position in the cascade. The energy generated by the small scale stack fuelled by artificial urine was used to power two different practical applications; an LED and a dc-motor driven windmil. This is a significant breakthrough and an important step into the future where collectives of MFCs can actually be used to operate real applications; in this particular study a total of 8mL (anode volume) was sufficient to charge a 2.5F capacitor, resulting in an energy transfer of 1.5J. For the sake of comparison, EcoBot-III was powered by 48x 6.25ml MFCs (300ml total anode chamber volume), each producing approximately 50  $\mu$ W and charging a 0.8F capacitor bank (Ieropoulos, Greenman & Melhuish, 2010a). Calculated on the average MPP of the MFCs in the cascade reported herewith, a theoretical projection suggests that only 30 of these 2ml small-scale MFCs (total volume 60ml) would theoretically be sufficient to operate EcoBot-III now. This emphasises the benefits of continuous flow miniaturised MFCs for maximising energy production from an abundant fuel source such as urine.

## FUTURE DIRECTIONS

The work described here is part of a larger study [funded by the Bill and Melinda Gates Foundation and the UK EPSRC](#) that is [also investigating the potential for the technology to kill pathogens and also produce clean water](#). –If in addition to generating electricity [as a result of cleaning up from](#) an abundant [waste product source](#), both these milestones can be achieved, then the future use of MFCs to globally benefit human-kind, is becoming a reality.

### Acknowledgements

[This work is funded by the Bill & Melinda Gates Foundation grant. no. OPP1044458 and the UK Engineering and Physical Sciences Research Council, grant no EP/I004653/1.](#)

## REFERENCES

- Brooks, T. & Keevil, C.W. (1997) A simple artificial urine for the growth of urinary pathogens. *Letters in applied microbiology*. 24 (3), 203–206.
- Degrenne, N., Buret, F., Allard, B., Bevilacqua, P. (2012) Electrical energy generation from a large number of microbial fuel cells operating at maximum power point electrical load. *Journal of Power Sources*. (205), 188–193.
- T Duncan (ed.) (1997) *Quantification of the Internal Resistance Distribution of Microbial Fuel Cells*. Second ed. London, John Murray Ltd.
- Fangzhou, D., Zhenglong, L., Shaoqiang, Y., Beizhen, X. & Hong, L. (2011) Electricity generation directly using human feces wastewater for life support system. *Acta Astronautica*. [Online] 68 (9-10), 1537–1547. Available from: doi:10.1016/j.actaastro.2009.12.013 [Accessed: 14 September 2012].
- Futamata, H., Bretschger, O., Cheung, A., Kan, J., Owen, R. & Neelson, K.H. (2012) Adaptation of soil microbes during establishment of microbial fuel cell consortium fed with lactate. *Journal of bioscience and bioengineering*. [Online] xx (xx), 1–6. Available from: doi:10.1016/j.jbiosc.2012.07.016 [Accessed: 13 September 2012].
- Harnisch, F. & Schröder, U. (2010) From MFC to MXC: chemical and biological cathodes and their potential for microbial bioelectrochemical systems. *Chemical Society reviews*. [Online] 39 (11), 4433–4448. Available from: doi:10.1039/c003068f [Accessed: 13 July 2012].

He, Z., Liu, J., Qiao, Y., Li, C.M. & Tan, T.T.Y. (2012) Architecture Engineering of Hierarchically Porous Chitosan/Vacuum-Stripped Graphene Scaffold as Bioanode for High Performance Microbial Fuel Cell. *Nano letters*. [Online] 12 (9), 4738–4741. Available from: doi:10.1021/nl302175j [Accessed: 20 August 2012].

[Ieropoulos, I. 2006. EcoBot: Towards an Energetically Autonomous Robot. PhD thesis. University of the West of England, Bristol, UK.](#)

Ieropoulos, I., Greenman, J. & Melhuish, C. (2010a) EcoBot-III: a robot with guts. In: *Proceedings of the Alfie XII conference*. 2010 Denmark.,. pp. 733–740.

Ieropoulos, I., Greenman, J. & Melhuish, C. (2010b) Improved energy output levels from small-scale Microbial Fuel Cells. *Bioelectrochemistry (Amsterdam, Netherlands)*. [Online] 78 (1), 44–50. Available from: doi:10.1016/j.bioelechem.2009.05.009 [Accessed: 9 September 2012].

Ieropoulos, I., Greenman, J. & Melhuish, C. (2008) *Microbial fuel cells based on carbon veil electrodes : Stack configuration and scalability*. [Online] (April), 1228–1240. Available from: doi:10.1002/er.

Ieropoulos, I., Greenman, J. & Melhuish, C. (2010c) Small Scale Microbial Fuel Cells and Different Ways of Reporting Output. *ECS Transaction*. 28 (9), 1–9.

Ieropoulos, I., Greenman, J. & Melhuish, C. (2012) Urine utilisation by microbial fuel cells; energy fuel for the future. *Physical Chemistry Chemical Physics*. [Online] 14 (1), 94. Available from: doi:10.1039/c1cp23213d [Accessed: 8 May 2012].

Ieropoulos, I., Winfield, J. & Greenman, J. (2010a) 2010\_Bioresource technol\_Effects of flow-rate inoculum and\_Ieropoulos.pdf. *Bioresource Technology*. 1013520–3525.

Ieropoulos, I., Winfield, J. & Greenman, J. (2010b) Effects of flow-rate, inoculum and time on the internal resistance of microbial fuel cells. *Bioresource technology*. [Online] 101 (10), 3520–3525. Available from: doi:10.1016/j.biortech.2009.12.108 [Accessed: 25 August 2012].

Ledezma, P., Greenman, J. & Ieropoulos, I. (2012) Maximising electricity production by controlling the biofilm specific growth rate in microbial fuel cells. *Bioresource technology*. [Online] 118615–618. Available from: doi:10.1016/j.biortech.2012.05.054 [Accessed: 16 August 2012].

Liu, X., Du, X., Wang, X., Li, N., Xu, P. & Ding, Y. (2012) Improved microbial fuel cell performance by encapsulating microbial cells with a nickel-coated sponge. *Biosensors & bioelectronics*. [Online] 1–4. Available from: doi:10.1016/j.bios.2012.08.014 [Accessed: 14 September 2012].

Logan, B.E. (2012) Essential Data and Techniques for Conducting Microbial Fuel Cell and other Types of Bioelectrochemical System Experiments. *ChemSusChem*. [Online] 5 (6), 988–994. Available from: doi:10.1002/cssc.201100604 [Accessed: 20 July 2012].

Qian, F. & Morse, D.E. (2011) Miniaturizing microbial fuel cells. *Trends in biotechnology*. [Online] 29 (2), 62–69. Available from: doi:10.1016/j.tibtech.2010.10.003 [Accessed: 2 August 2012].

Russell, J.B. (2007) The energy spilling reactions of bacteria and other organisms. *Journal of molecular microbiology and biotechnology*. [Online] 13 (1-3), 1–11. Available from: doi:10.1159/000103591 [Accessed: 4 August 2012].

- Winfield, J., Ieropoulos, I. & Greenman, J. (2012) Investigating a cascade of seven hydraulically connected microbial fuel cells. *Bioresource technology*. [Online] 110245–250. Available from: doi:10.1016/j.biortech.2012.01.095 [Accessed: 12 September 2012].
- Yu, J., Park, Y., Cho, H., Chun, J., Seon, J., Cho, S. & Lee, T. (2012) Variations of electron flux and microbial community in air-cathode microbial fuel cells fed with different substrates. *Water science and technology : a journal of the International Association on Water Pollution Research*. [Online] 66 (4), 748–753. Available from: doi:10.2166/wst.2012.240 [Accessed: 6 August 2012].
- Zhang, G., Wang, K., Zhao, Q., Jiao, Y. & Lee, D.-J. (2012a) Effect of cathode types on long-term performance and anode bacterial communities in microbial fuel cells. *Bioresource technology*. [Online] 118C249–256. Available from: doi:10.1016/j.biortech.2012.05.015 [Accessed: 19 June 2012].
- Zhang, J., Zhang, E., Scott, K. & Burgess, J.G. (2012b) *Enhanced Electricity Production by Use of Reconstituted Artificial Consortia of Estuarine Bacteria Grown as Biofilms*.